A large acceptance scintillator detector with wavelength shifting fibre read-out for search of eta-nucleus bound states

The GEM Collaboration: M.G.Betigeri [a], P.K.Biswas [b], A. Budzanowski [c], A. Chatterjee [a], R. Jahn [d], S.Guha [b], P.Hawranek [e], B.K.Jain [n], S.B.Jawale [b], V. Jha [a,*] , K. Kilian [f], S. Kliczewski [c], Da. Kirillov [f], Di. Kirillov [g], D. Kolev [h], M. Kravcikova [i], T. Kutsarova [j], M. Lesiak [f], J. Lieb [k], H. Machner [f,o], A. Magiera [e], R. Maier [f], G. Martinska [ℓ], S. Nedev [m], N. Piskunov [g], D. Prasuhn [f], D. Protić [f], J. Ritman [f], P. von Rossen [f], B. J. Roy [a], P. Shukla [a], I. Sitnik [g], R. Siudak [c,f], R. Tsenov [h], M. Ulicny [ℓ], J. Urban [ℓ], G. Vankova [f,h]

[a] *Nuclear Physics Division, BARC, Mumbai-400 085, India*

[b] *Centre for Design and Manufacture, BARC, Mumbai-400 085, India*

[c] *Institute of Nuclear Physics, Polish Academy of Sciences, Krakow, Poland*

[d] *Helmholtz-Institut für Strahlen- und Kernphysik der Universität Bonn, Bonn, Germany*

[e] *Institute of Physics, Jagellonian University, Krakow, Poland*

[f] *Institut für Kernphysik, Forschungszentrum Jülich, Jülich, Germany*

[g] *Laboratory for High Energies, JINR Dubna, Russia*

Preprint submitted to Nucl. Instr. and Meth. in Phys. Res. A 21 January 2014

[h] *Physics Faculty, University of Sofia, Sofia, Bulgaria*

[i] *Technical University Kosice, Kosice, Slovakia*

[j] *Institute of Nuclear Physics and Nuclear Energy, Sofia, Bulgaria*

[k] *Physics Department, George Mason University, Fairfax, Virginia, USA*

[ℓ] *P. J. Safarik University, Kosice, Slovakia*

[m] *University of Chemical Technology and Metallurgy, Sofia, Bulgaria*

[n] *Physics Department, Mumbai University, Vidyanagari, Mumbai*

[o] *Fachbereich Physik, Universität Duisburg-Essen, Duisburg, Germany*

Abstract

A large acceptance scintillator detector with wavelength shifting optical fibre readout has been designed and built to detect the decay particles of η-nucleus bound system (the so-called η-mesic nuclei), namely, protons and pions. The detector, named as ENSTAR detector, consists of 122 pieces of plastic scintillator of various shapes and sizes, which are arranged in a cylindrical geometry to provide particle identification, energy loss and coarse position information for these particles. A solid angle coverage of $\sim$95% of total 4π is obtained in the present design of the detector. Monte Carlo phase space calculations performed to simulate the formation and decay of η-mesic nuclei suggest that its decay particles, the protons and pions are emitted with an opening angle of $150^\circ \pm 20^\circ$, and with energies in the range of 25 to 300 MeV and 225 to 450 MeV respectively. The detailed GEANT simulations show that $\sim$ 80 % of the decay particles (protons and pions) can be detected within ENSTAR. Several test measurements using alpha source, cosmic-ray muons etc. have been carried out to study the response of ENSTAR scintillator pieces. The in-beam tests of fully assembled detector with proton beam of momentum 870 MeV/c from the Cooler synchrotron COSY have been performed. The test results show that

the scintillator fiber design chosen for the detector has performed satisfactorily well. The present article describes the detector design, simulation studies, construction details and test results.

Key words: Scintillator detector; WLS optical fibre read-out; Eta-nucleus bound states

1 Introduction

A large acceptance plastic scintillator detector ENSTAR has been designed and built for studies of η-mesic nuclei - a bound system of η-meson and a nucleus. The finding of strong and attractive nature of the η-nucleon(η-N) scattering length and the presence of a resonance near the η-N threshold, provide an interesting possibility of the formation of η-nucleus bound states [1,2]. The experimental confirmation of the existence of such bound systems would open up new avenues for elucidation of the η-nucleus dynamics at intermediate energies. Such experiments [3] are being performed at the intermediate energy accelerator facility COSY Jülich, using GeV energy proton beam. The experiments use recoil-free transfer reactions p+(^{Z}X$_{A}$) $\rightarrow$ ^{3}He + $(^{Z-1}X_{A-2})_{\eta}$ on several target nuclei X = Li, C, Al, etc. The expected cross section for events corresponding to formation of η-mesic nuclei is rather low, hence, a dedicated detection system is needed to enhance the sensitivity of the measurement. ENSTAR is the part of detection system which has been developed in order to obtain an unambiguous signal for the formation and decay of the η-nucleus

* Corresponding author. Nuclear Physics Division, BARC, Trombay, Mumbai-400085, India. Tel:++91-22-25593457; Fax: ++91-22-25505151.
Email address: vjha@barc.gov.in (V. Jha).

bound state. The outgoing ^{3}He particles are detected in the Big Karl detection system [4,5], which includes a magnetic spectrograph and its focal plane detectors consisting of drift chambers and scintillator hodoscopes. The corresponding proton and pion from the decay of η-mesic nucleus are registered in ENSTAR. In addition to the η-bound states search, the ENSTAR detector can also be used in many other experiments where the missing mass determination of the reaction product needs to be done in coincidence with its decay products e.g., for the study of Δ interaction in nuclear matter, where the decay products of Δ states, protons and pions can be detected by ENSTAR [6]. The details of the Big Karl spectrometer have been reported elsewhere [4,5]. In this paper, the description of the newly built ENSTAR detector is reported. The geometric design, simulation studies and fabrication procedure are described. Test measurements done at various stages during the construction of ENSTAR as well as the in-beam tests performed at the COSY accelerator are presented.

2 Physics background and ENSTAR design considerations

Phase space calculations to simulate eta-mesic nucleus decay events were performed using the N-body Monte-Carlo event generator program "Genbod" [7]. The program generates multi-particle weighted events according to Lorentz invariant Fermi phase space. The reaction p+^{16}O $\rightarrow$ ^{3}He+$^{14}N_\eta$ was studied at a momentum close to the magic momentum. The magic momentum is defined as the beam momentum at which recoil-less η can be produced in the elementary process. For the reaction considered, the elementary reaction is pd $\rightarrow$ ^{3}Heη, for which the magic momentum was calculated to be 1.745 GeV/c, corresponding to a proton kinetic energy of T_p=1.05 GeV. The η-nuclei for-

mation proceeds through the excitation of N^* (1535 MeV) resonance and one of its decay channels is through proton and pion. The simulations were performed in two steps. In the first step, Monte Carlo events were generated for the p+^{16}O $\rightarrow$ ^{3}He+$^{14}N_{ex}$ reaction where an excitation energy of 547 MeV, equal to the mass of eta meson, is given to ^{14}N nucleus. Only those ^{14}N events were considered for which the corresponding ^{3}He particle is within the Big Karl acceptance ($\theta_{lab}(^3\mathrm{He}) \leq 6^\circ$). In the next step, the decay of N^* to p-π pair was simulated. The mass of N^* was taken equal to the mass of a nucleon plus the mass of an eta meson, while its velocity was assumed to be the same as that of the recoil ^{14}N modified by the Fermi momentum distribution. The p-π opening angle distribution shows a peak at around $\approx$150° with a width of 40° (Fig. 1). The energy spectrum for the proton peaks at T_p $\approx$100 MeV with a width (FWHM) of 120 MeV (Fig. 2), while the pion spectrum has a peak at $\approx$320 MeV and a similar width(Fig. 3) as that of proton peak. The simulations were also carried out for other eta-mesic nuclei formation reactions on different target nuclei. The energy spectra and opening angle distributions were found to be similar as that in the previous case.

A detector employing plastic scintillators in the ΔE - E configuration, which provides the particle identification and energy information of the measured particles, has been chosen for the present design. The thickness of the detector elements has been designed to stop the decay protons and obtain a good signal for pions, keeping in mind the space constraints around the detector in the experimental area. The detector has been segmented in both θ and ϕ direction for obtaining position information with the desired granularity. Large solid angle coverage has been achieved by minimising any unwanted material

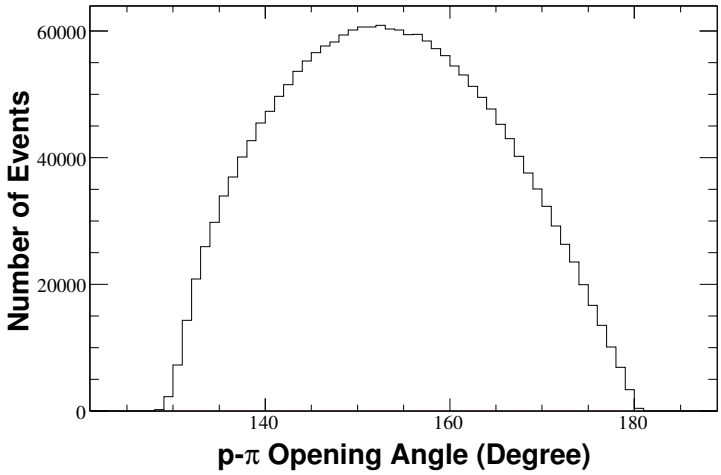

Fig. 1. The p-π opening angle distribution for η-mesic nucleus decay particles obtained from Monte-Carlo phase space calculations as detailed in the text.

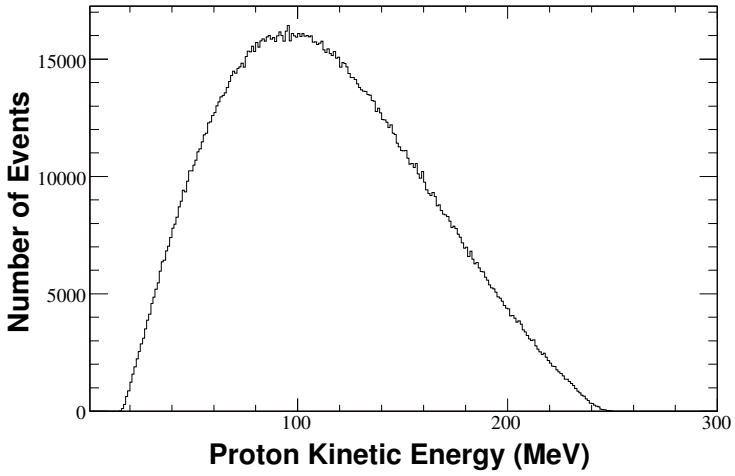

Fig. 2. Kinetic energy distribution of protons from η-mesic nucleus decay obtained from Monte-Carlo phase space calculations.

within the detector.

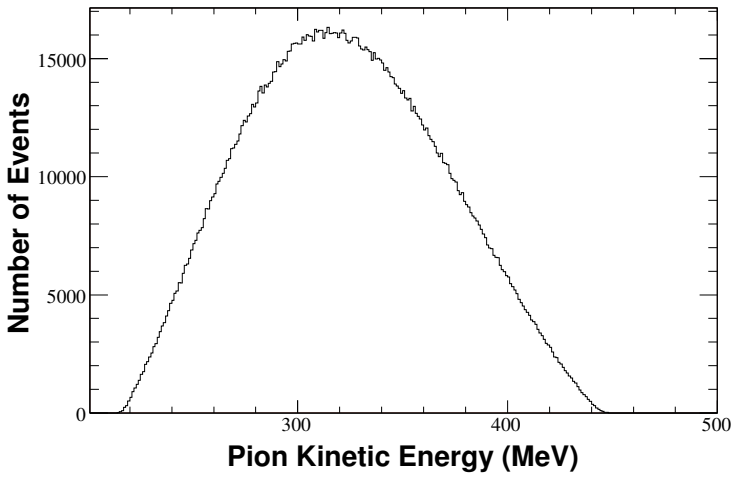

Fig. 3. Kinetic energy distribution of pions from η-mesic nucleus decay obtained from Monte-Carlo phase space calculations.

3 Design details and fabrication

3.1 Detector geometry

Based on the design and geometric criteria, ENSTAR is cylindrically shaped with three layers of plastic scintillators. These layers are used to generate $\Delta E - E$ spectrum for particle identification and to obtain total energy information for the stopped particles. Each layer is divided into a number of pieces to obtain θ and ϕ information. The detector, which is made up of two identical half cylinders, is assembled around a scattering chamber of 1.5 mm thick carbon compound fibre material. The scattering chamber as shown in Fig. 4 is designed in a "T" shape with a thin target pipe projecting out from the middle of beam pipe. The two half cylinders of the detector are placed on either side of the target pipe. The target pipe has sufficient space from inside to enable mounting of solid targets. A Liquid target chamber, similar to the one existing at COSY laboratory can also be used after some modifications. The angular

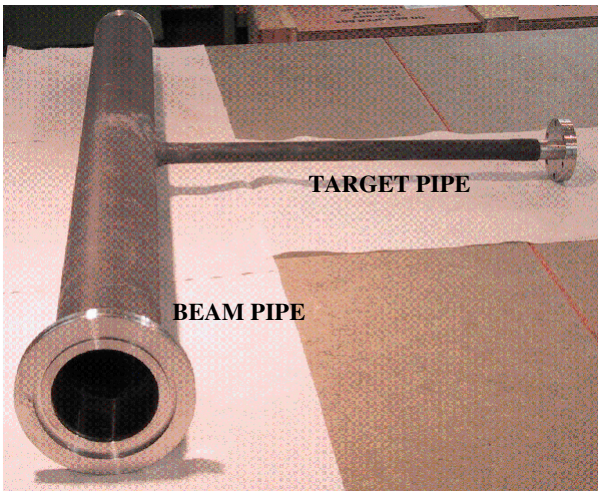

Fig. 4. Photograph of the scattering chamber made from the carbon fibre material. It consists of a beam pipe and a thin target pipe for inserting a target ladder.

coverage of the detector is $\theta_{lab} = 15^o - 165^o$ in the θ-direction, while its cylindrical geometry ensures an azimuthal angle coverage of $\phi = 0^o - 360^o$. With the present design, the detector provides a solid angle coverage of ∼95% of 4π. An assembly drawing of ENSTAR together with its sectional view through the target is shown in Fig. 5. A total of 122 pieces of scintillators of different shapes and dimensions are used to give three concentric cylindrical layers on assembly.

The inner layer is used to provide the energy loss and ϕ information of the particles passing through it and is designed as two hollow plastic scintillator cylinders with the following dimensions; Inner diameter(ID) = 84 mm, Outer diameter(OD)=96 mm and a length of 390 mm. Both the cylinders are split into eight equal sectors with a sector angle equal to 45^o. Thus the inner layer consists of a total of 16 segmented annuli each of which is read out separately. A ϕ resolution of 45^o is satisfactory for the studies on η -mesic nuclei, as the decay particles are emitted with a very large opening angle between them.

Signals from the middle layer are used to obtain energy and θ information. This layer consists of seven identical scintillator bars in both the halves, each in the form of an isosceles triangle with base = 243.1 mm and height = 152.4 mm arranged to form an annular cylinder of ID=100 mm, OD= 449.4 mm and length = 390 mm in each half. Each of triangular bars (390 mm long) is further split lengthwise into six pieces of length 13 mm, 16 mm, 21 mm, 37 mm, 213 mm, and 90 mm so that each piece covers an angle interval of $\Delta\theta_{lab}$ equal to 15^o. A total of 84 pieces of scintillators are used for the middle layer cylinder. The geometrical granularity allows an angular resolution of $\Delta\theta_{lab}$ equal to 15^o. In conjunction with signals from middle layer, signals from the outer layer are expected to provide an unambiguous signal for pions. The outer layer consists of a total of 22 identical bars, each 390 mm long and a cross section of an isosceles triangle with base = 328.3 mm and height = 105.5 mm. These outer layer pieces form an annular cylinder of ID = 453.5 mm, OD = 692.5 mm. Thus, with two identical cylinders on either side of the target for all the three layers, the detector provides an angular coverage of $15 \leq \theta_{lab} \leq 165^o$ in the θ-direction and almost full coverage in the ϕ-direction.

3.2 GEANT simulation

GEANT [8] calculations have been carried out by simulating the conditions of the real experiment to simulate the ENSTAR detector's response to eta-nucleus decay particles, namely, protons and pions. The detector geometry has all its 122 pieces arranged around the scattering chamber. The target has been positioned at the centre of the detector, inside the scattering chamber which

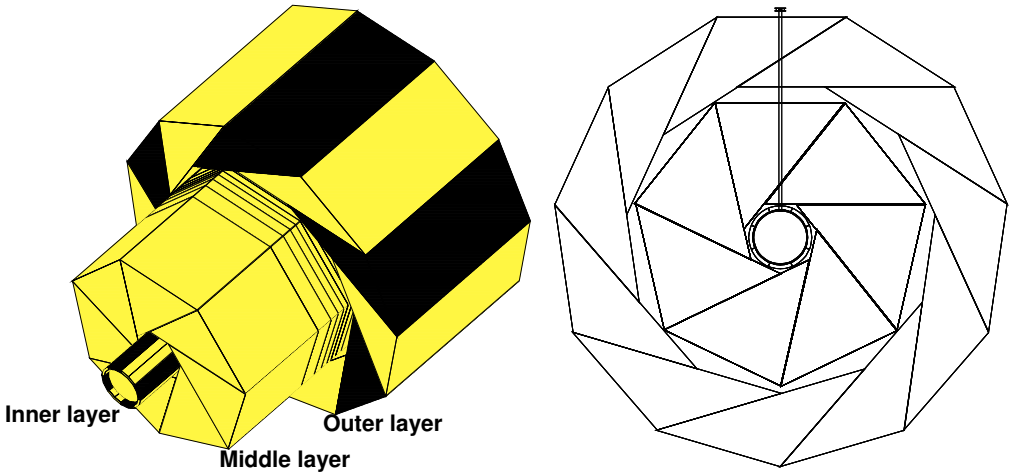

Fig. 5. Left part : An assembly drawing of ENSTAR detector is shown. Some pieces of the middle and outer layers are moved out for an inside view. Detailed dimensions are given in the text. Right part : A Sectional view of the detector through the target is shown. Beam pipe along with the target pipe attached to it, is also drawn.

is in vacuum. The existing gap between the various layers of ENSTAR is filled with air. The η-mesic nucleus decay events are produced in a collision of 1.05 GeV proton beam with a target. A Monte Carlo event generator as detailed in section 2 is used to simulate such events. The protons are stopped in the detector while pions, as expected, pass through it giving only partial energy loss in the detector. Fig. 6 shows a two dimensional plot of energy loss in the first layer versus total energy loss in the detector. The response of various layers of ENSTAR for protons and pions from such events have been investigated. The present design does not plan to obtain full energy information of pions, however, as desired a mass separation of pions from protons can be achieved. From the particle selection in the ΔE-E two-dimensional spectrum of Fig. 6, the decay events detected within the detector can be estimated. It is found that the 80 % of total protons and pions generated can be identified from the ΔE-E spectrum. It is further clear from the figure that the energy loss for most of pions is in the 50-100 MeV range , where a clear separation

between protons and pions can be achieved. The separation of pions from the protons could be difficult in the higher energy loss region of pions. However the fraction of the pion events in the energy range of 100-250 MeV is less compared to number of events in the low energy range.

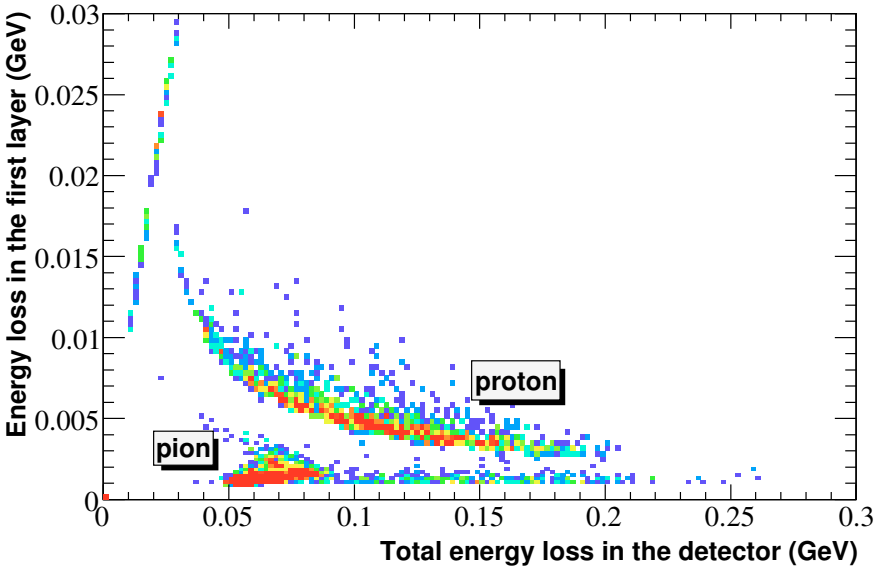

Fig. 6. A two dimensional plot of ΔE (energy loss in the inner layer) vs E + ΔE (energy loss in all the layers) showing the particle separation in ENSTAR. The results are obtained from GEANT simulations for the events from the η-mesic nucleus decay.

3.3 Scintillator grooving and fibre coupling

Plastic scintillators, having the properties equivalent to Bicron BC-408 series, were procured from Scionix Ltd, Netherlands [9], for the fabrication of detector elements. The use of light guides for scintillator read out was not practicable due to the complicated geometry of the detector. The idea of using wave-

length shifting (WLS) optical fibres for scintillator read out was invoked for the present detector. Earlier studies[10,11] have shown that the double-clad fibres give better light yield (70% more light) than comparable single clad ones, due to an increase in the fraction of light that undergoes total internal reflection. The double-clad WLS optical fibres having 1mm diameter were used for light transport. A number of grooves for fixing fibres to the scintillators were made on the surface of scintillators . The middle and outer layer pieces were machined for 19 grooves each having 4 mm width and 1.5 mm depth. The grooves cover roughly 40 % of the area of one face of scintillator. For the inner layer pieces, 15 grooves of 1.0 mm width and 1.5 mm depth were machined with a spacing of 1.5 mm. The machining was done at the Central Workshop, BARC using a computer controlled 4 mm (1mm for the grooves on inner layer pieces) carbide cutter (End-Mill). A suitable cooling arrangement with chilled air was used in order to avoid any local heating. Each piece of middle and outer layer has 76 fibres placed in 19 grooves (4 fibres in each groove), while each inner layer piece has 15 fibres (1 fibre in each groove. The scheme of fibre scintillator coupling is illustrated in Fig. 7 for a typical middle layer scintillator piece.

The total amount of fibre used was 7.8 km in length. The fibre length for each scintillator pieces was decided on the basis of availability of space in the experimental area. While the length of fibre should not be very long in order to minimise attenuation losses, its bending radius should also be kept high. The conventional minimum bending radius of these fibres is ten times the fibre diameter. Bending fibres below this radius may result in significant light loss due to damage in mechanical as well as optical properties. The length

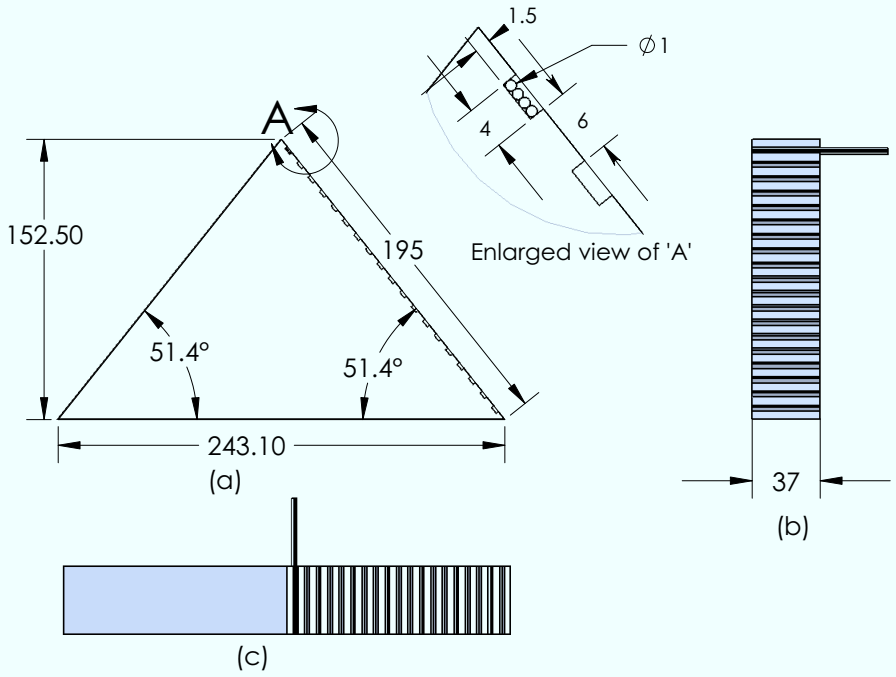

Fig. 7. The sketch diagram of a typical middle layer scintillator piece showing the grooves and fibre alignment details. There are 19 grooves on one face of this triangular bar with four fibers placed inside each groove. The alignment of fibres with the scintillator is shown in (b) and (c). For illustration purposes fibres in only one groove are drawn.

of fibres for each scintillator piece was optimized accordingly. Since the light readout is from one end of the fibres only, the light traversing to the other end must be reflected back. Therefore, before fixing the fibres, a highly reflective anodized aluminum sheet (known as EverBrite [12]) was placed on one face of the scintillator and held in place with aluminized mylar tape. A good surface finish and polished fibre ends are essential to prevent light losses at both the reflecting as well as at the readout interface . This has been achieved by different techniques. The cutting and polishing of fibres for the middle and outer layer pieces were done before fixing them to the scintillators. For polishing, many fibres were grouped together in bundles inside a perspex tube. The fibre face was cut along with the perspex by a diamond tipped cutting tool

giving a surface finish of 0.7 μm. The final polishing of these fibres was done with 0.3 μm size alumina powder on velvet cloth. The polished fibres were fixed in the scintillator grooves with the Bicron 600 optical cement at few locations along the grooves. However, to give an additional holding strength, five-minute epoxy was used wherever necessary. It is preferable to use the Bicron cement as it has the same refractive index as that of the scintillator and its light transmission above 400 nm wavelength is more than 98 %. In addition, aluminized mylar tape was also used at few places for holding the fibres. For the inner layer pieces, a different method was followed. First, the fibres were fixed in the grooves using Bicron cement with a small amount of five-minute epoxy glue at the ends of the fibre-scintillator joint. This end of the scintillator along with the fibres were then polished for all 16 inner-layer pieces. This was done at the optics workshop of the Spectroscopy Division, BARC by the lapping technique. Fine alumina powder of 20 μm, 12 μm and 6 μm were used in successive stages of lapping. The final finishing was then achieved by polishing with diamond paste and alumina of 1 μm and 0.3 μm sizes giving a surface finish of 0.3 μm. Fig. 8 (left part) shows the polished end of one of the scintillator pieces. Finally the highly reflective EverBrite sheet was placed at this polished end (not shown in the figure) for light reflection. The other open end of all the fibres of individual scintillator pieces were bundled together and then glued to the inside of a 2.54 mm diameter perspex tube - known as "cookie" [11] (a cylindrical piece of acrylic, matching the photo multiplier tube in diameter). This end of fibres were polished along with the cookie. The fibres along with the cookies were diamond polished by diamond paste and alumina powder. Fig. 8 (middle picture) shows some of the finished (except for its covering by black foil) inner layer pieces with fibres and cookie attached. One of the middle layer piece is also shown in Fig. 8(right picture).

The cookie end was coupled to the photo-multiplier tube for conversion of the light signal into photo-electrons which were then processed electronically. In order to reduce light losses from scintillators, the scintillator elements were wrapped with tyvek, a paper-white reflecting foil made of polyethylene[13]. The wrapping by tyvek, apart from light reflection, also helps in minimising the cross-talk. All the detector pieces were finally covered by black tedlar foil for light tightness and reducing the cross-talk among various detector elements.

Fig. 8. Photograph of some inner and middle layer pieces of ENSTAR while being fabricated. Left part shows inner layer pieces with fibres inside scintillator grooves while the middle part shows the some of the similar pieces after it has been covered with the Tyvek paper. At the other end fibres from each piece are bundled together and coupled to a"cookie". In the right part of the figure one of the middle layer pieces with fibres placed inside the grooves is shown.

3.4 Scintillator readout details

The Bicron optical fibre BCF-91A, used in the present detector for collecting light produced in the scintillator volume has an emission spectrum in the visible green region. In order to have an efficient readout of this light, the photomultiplier tubes (PMTs) that have a spectral response extending into

the green region and which match the light emission characteristic of the wave length shifting fibres were selected. The PMTs are of the 9112B series manufactured by Electron Tubes Ltd (ETL), United Kingdom [14]. The PMTs are of 25 mm diameter with Rubidium bialkali photocathode having an enhanced green sensitivity. A total of 122 photomultiplier tubes are used for the readout of ENSTAR. The PMTs have a current amplification of 10^6 and a dark current of less than 10 nA. The tubes are fast and have a rise time of less than 3 ns. The PMTs, during the experiment, were covered by μ-metal sheets which have also been procured from ETL, UK. The base of the PMTs i.e., voltage dividers are also made by the same manufacturer. Special aluminum holders were fabricated for holding the PMTs and cookies together.

3.5 Detector assembly

The pieces of the inner layer of the detector are the lightest ones and were easy to mount. They were simply held around the beam pipe/target chamber with tape. The other pieces of ENSTAR i.e., middle and outer layer pieces are relatively heavier and special support structures were designed and built for holding these pieces in place. The basic supporting structure, which is mostly an exoskeleton, was made from hylam (low Z material) plates. Due to the compact geometry of the detector no support structure was needed inside the sensitive volume of the detector, except only at few places in the space between the middle and the outer layer where three support strips made of hylam have been put in each half of the detector. These support strips were joined by aluminum rings on both ends for the middle layer. The simulations were repeated with and without the hylam strips (acting as inactive material

inside the detector). An acceptance loss of less than $\sim 1\%$ for the particles to be detected is predicted. For the outer layer, the hylam plates were joined by aluminum brackets at both ends. The detector after assembly was placed on a stainless steel stand which was fixed on a movable trolley made from angle-iron. A stand to hold PMTs was also constructed and integrated in the same support structure. Fig. 9 shows a photograph of ENSTAR detector along with its support structure mounted at the COSY beam line.

Fig. 9. A photograph of the ENSTAR detector mounted at the COSY beam line along with its support structure and the stand which has been used to transport the detector to the beam line.

4 Test Measurements

A number of test measurements were performed during the construction and commissioning of the detector. A light-tight black box was constructed for the preliminary tests of the phototubes and the scintillator pieces. The PMTs and its bases were tested to check for their proper functioning and to determine their optimum operating voltage. The variation of signal pulse height from a

scintillator tile was studied as a function of number of fibres. The pulse height, which depends on the amount of light collected by the fibres, is observed to increase with the increase in the number of fibres and saturates when fibre covers about 30 - 40% of the scintillator tile surface. The number of fibres for each scintillator tile has been optimized accordingly. The light output of different pieces of ENSTAR was also tested with an alpha source for which a simple test setup was constructed.

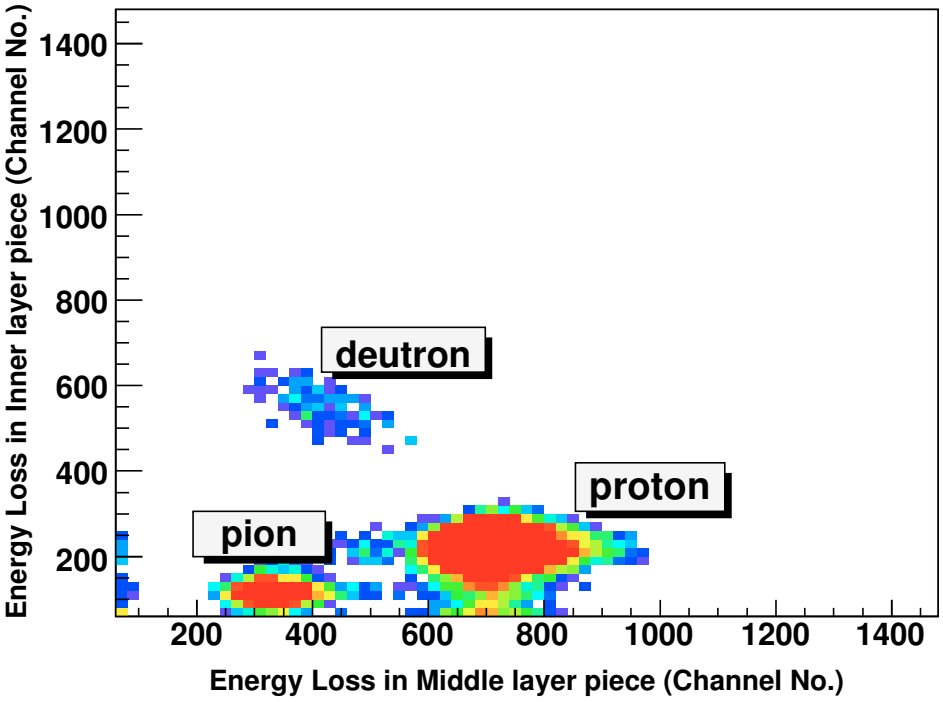

Fig. 10. A two dimensional spectrum of the energy losses in inner and middle layer pieces of ENSTAR mounted at the focal plane exit of Big Karl magnetic spectrograph in ΔE1 - ΔE2 configuration. The spectrum shows the pions, protons and deutrons of energies $\sim$430 MeV, $\sim$ 150 MeV and $\sim$ 80 MeV respectively, which are selected by a BigKarl momentum setting of 550 MeV/c.

The first in-beam test at COSY was performed by mounting a few pieces of ENSTAR from the inner and middle layers arranged in a ΔE1 - ΔE2 configuration at the exit of the focal plane of the magnetic spectrograph BigKarl. A proton beam of momentum 1.54 GeV/c, corresponding to kinetic energy of 865 MeV, was bombarded on a thick Alumina target. The spectrograph BigKarl was set for different momenta to select various energies of protons from 35 to 225 MeV and pions in the range of 150 to 560 MeV. Fig. 10 shows the ΔE1-ΔE2 energy spectrum of various particles detected in scintillator pieces for a typical BigKarl momentum setting of p/q=550 MeV/c. A Good separation among all particle groups (e.g. pions, protons, deuterons etc.) was obtained. The particle identification was confirmed from the time of flight information, which was measured simultaneously between two hodoscopes layers placed at a distance 4m apart at the focal plane of BigKarl.

The final test measurement of ENSTAR in fully assembled condition was performed using a proton beam of momentum 0.870 GeV/c at COSY. In addition to light-output test of all scintillator pieces, a study of the relative gain of various elements and absolute calibration was performed. Several nuclear reactions (pp elastic scattering, $pp \rightarrow d\pi^+$, proton impinging on a heavy target etc.) were used for this purpose. Coincidence data i.e. a 2-fold coincidence between different elements of ENSTAR were collected. In addition, cosmic-ray data were also recorded with good statistics.

In the pp elastic scattering measurement scattered protons having energies from 25 to 340 MeV are detected in the forward half of the detector. In this case, the trigger was made from the events which have a double hit in the

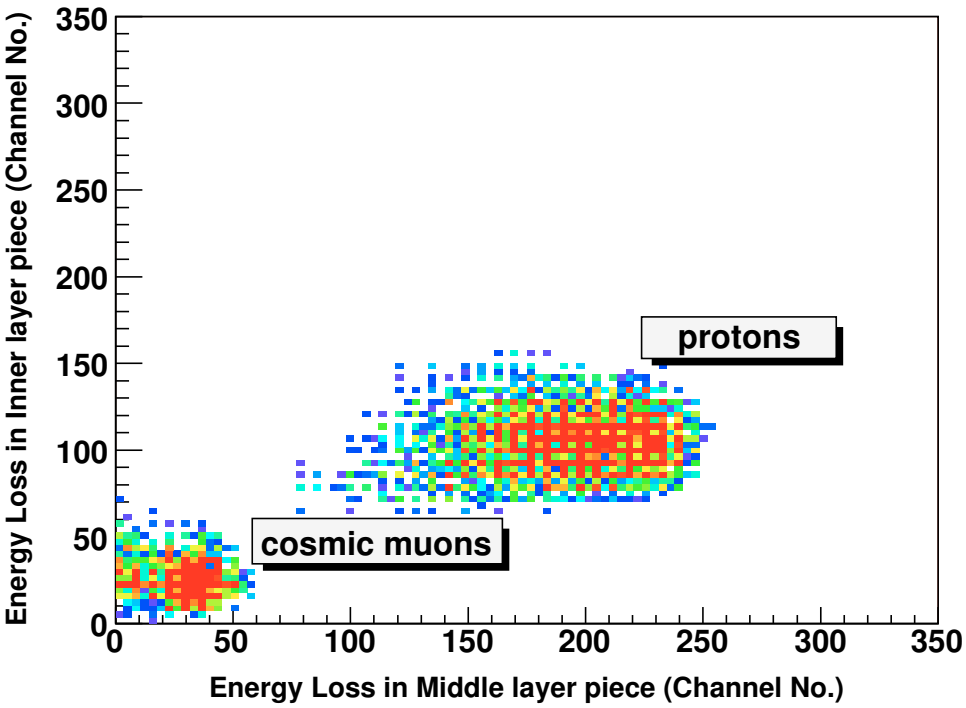

Fig. 11. A two dimensional spectrum of one of the inner layer piece vs the corresponding middle layer piece of ENSTAR for protons in the energy range of 225-330 MeV obtained from pp elastic scattering data. Cosmic ray data from a different run are also shown in the same figure.

296 inner layer and at least a single hit in the middle layer. In addition, the condi-
297 tion of co-planarity of the elastically scattered proton pair was ensured. Light
298 output of one of the inner-layer scintillator piece versus the corresponding
299 middle-layer scintillator piece is plotted in Fig. 11. The proton band shown
300 in the figure corresponds to an energy range of $225 - 330$ MeV. A band cor-
301 responding to cosmic muons is also shown in the figure which was obtained
302 from cosmic-ray data collected separately in a different run, as described later
303 in the text.

304

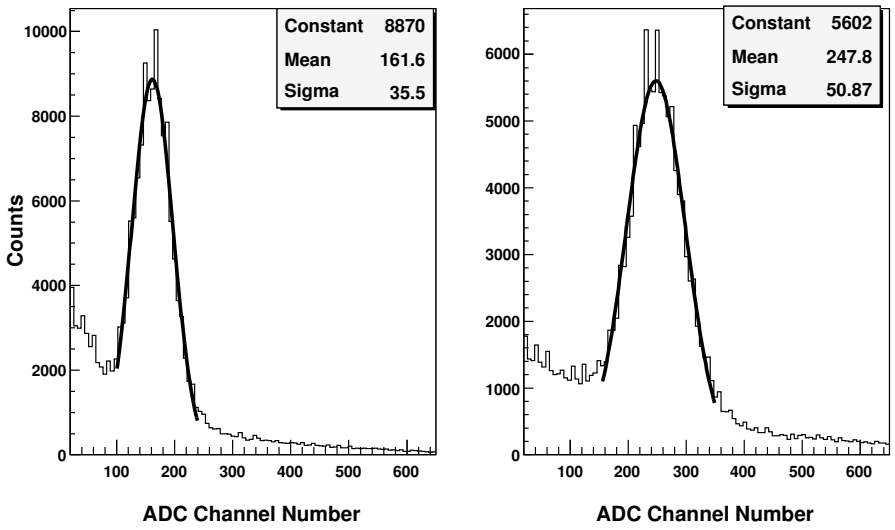

Fig. 12. ADC spectra of two adjacent middle layer scintillators uniformly illuminated in ϕ- direction by scattered particles from beam impinging on a thick target kept in front of detector. Peak positions are used to get the relative gains of various pieces in ϕ-direction.

The relative gain calibration among different scintillator pieces covering the same θ- but different ϕ-ranges is achieved using reactions in which protons are incident on a thick heavy target. In this case the target, instead of its conventional location which is at the centre of ENSTAR, was placed at a position where the beam enters the detector, Scintillators of the same shape and dimensions form an annular cylindrical ring and therefore, are uniformly illuminated by the scattered particles. The relative gain for the different elements of the ring is obtained from the peak positions of the spectra shown in Fig. 12. For measurements with the cosmic-rays, two additional scintillator hodoscope paddles were placed just above and below the ENSTAR scintillator element being tested. Signals from these paddles formed the cosmic-ray trigger. ADC spectra from two adjacent scintillators of the middle layer for the cosmic data are shown in Fig. 13 (left and middle part). The extreme right part of the

figure is a pedestal subtracted ADC spectrum generated from combination of these two spectra using the relative gain between the corresponding two pieces as determined above. The triangular shape of middle layer(as well as outer layer) scintillators and the present detector geometry allow a selection of an overlap portion between two adjacent scintillators such that muons travel a constant thickness of 150 mm. The centre of the peak corresponds to an average energy loss of ∼27 MeV since a minimum ionizing particle typically loses ∼1.8 MeV per cm of plastic scintillator [15]. This method was used to extract the absolute gain calibration of all the middle and outer layer scintillator pieces.

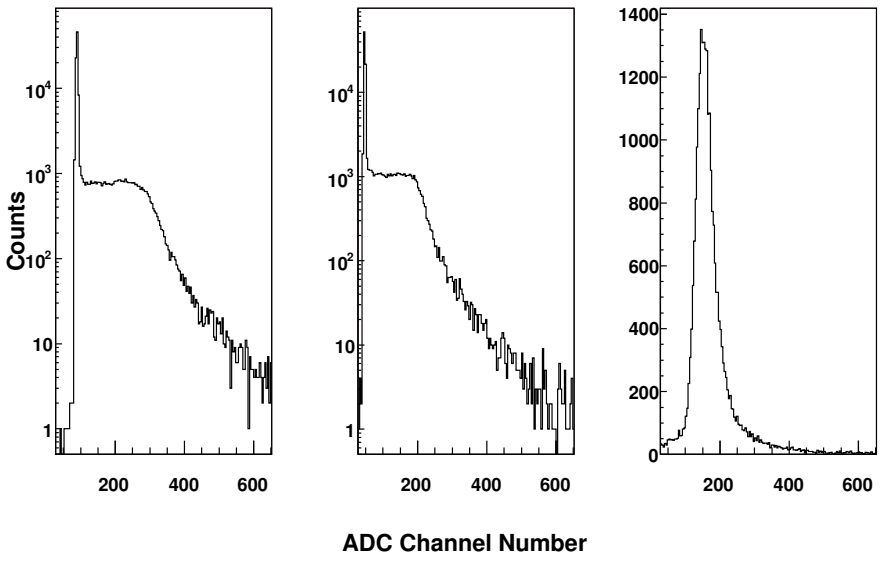

Fig. 13. ADC spectra from two adjacent middle layer scintillators for cosmic ray data. The extreme right part of the figure is generated by demanding an overlapping geometry condition such that cosmic muons travel a constant thickness. See text for details.

5 Conclusions

We have presented a detailed description of a large acceptance scintillator detector ENSTAR, which has been designed and constructed for studying the production and decay of η-nucleus bound systems, the η-mesic nuclei at the multi-GeV hadron facility COSY. Monte Carlo phase space calculations to simulate the formation and decay of eta-mesic nucleus predict an energy range of 25 to 250 MeV for the decay protons and energies from 250 to 500 MeV for the decay pions. The detector is cylindrically shaped in three layers and is segmented into a number of pieces for the detection of η-mesic decay events. GEANT simulations predict a clear mass separation between the protons and pions based on the energy loss information in different layers. A number of test measurements have been performed to test the performance of the individual components of the detector. Some of the scintillator pieces have been tested at COSY by placing them in $\Delta E1 - E2$ configuration at the exit of focal plane detection system of the magnetic spectrometer BigKarl. These scintillator pieces have been tested with protons in the energy range of 35-200 MeV and pions in 150-500 MeV energy range selected from the Big Karl. The detector has been further tested in fully assembled condition, using 870 MeV/c proton beam from COSY, Jülich. In addition, the measurements using the cosmic muons have been also performed. For the test measurement with 870 MeV/c proton beam, the elastically scattered protons having energy in 25-340 MeV range, were detected in ENSTAR. A satisfactorily good detector response is obtained with the elastic protons as well as the cosmic muons.

Acknowledgements

This work has been part of the Indo-German bilateral agreement. We are thankful to the International Studies Division, DAE, India. Our sincere thanks goes to Dr.S.S.Kapoor and Dr.S.Kailas, BARC for their interest and support throughout this project. We are thankful to Prof. N. K. Mondal, TIFR, Mumbai for many useful discussions and supply of EverBrite sheets. We are indebted to the technical staff of the Centre for Design and Manufacture, BARC, Spectroscopy Division, BARC and Institute of Nuclear Physics, Forschungszentrum, Jülich for their assistance. We would like to acknowledge the support from the European community research infrastructure activity under the FP6 "Structuring the European Research Area" programme under the contract no.RII3-CT-2004-506078.

References

[1] L. C. Liu and Q. Haider, Phys. Rev. C 34 (1986) 1845.

[2] R.S. Bhalerao and L.C. Liu, Phys. Rev. Lett. 54 (1985) 865.

[3] H Machner et al., GEM Collaboration, COSY-Proposal No 50, FZ Jülich, 2000.

[4] Siegfried A. Martin et al, Nucl. Instr. and Meth. 214 (1983) 281.

[5] Betigeri M. et al. GEM collaboration, Nucl. Instr. Meth. A 487 (2002) 314.

[6] A. Gillitzer et al., COSY-Proposal No 96, FZ Jülich, 2000.

[7] F.James , GENBOD - CERN Program Library write up no. W515.

[8] R. Brun et al, GEANT - CERN Program Library W5013.

[9] SCIONIX plastic scintillators, SCIONIX, http://www.scionix.nl

[10] M. Adams et. al., D0 collaboration, Nucl. Inst. and Meth. A 366, (1995) 263.

[11] B. S. Acharya et. al., D0 Collaboration, Nucl. Inst. and Meth. A 401, (1997) 45.

[12] EverBrite anodized aluminium, Alcoa Brite Products Inc., 3040, Northwood Parkway, Norcross, GA 30071.

[13] Tyvek and Tedlar TCC 15BL3, DuPont de Nemours Int. SA, Switzerland.

[14] ETL Photo multiplier tubes, Electron Tubes Ltd., http://www.electron-tubes.com.

[15] C.P.Achenbach et al., Nucl. Inst. Meth. A 539 (2005) 112